Research on Chemical Intermediates (2023) 49:289–305
https://doi.org/10.1007/s11164-022-04861-z

An in situ study of the thermal decomposition of 2,2′-azobis(2-methylpropionitrile) radical chemistry using a dual-mode EPR resonator

Giuseppina Magri[1] · Michael Barter[2] · Jack Fletcher-Charles[1] · Heungjae Choi[2] · Daniel Slocombe[2] · Emma Richards[1] · Andrea Folli[1] · Adrian Porch[2] · Damien M. Murphy[1]

Received: 23 September 2022 / Accepted: 22 October 2022 / Published online: 12 November 2022

Abstract

A custom-built dual-mode EPR resonator was used to study the radical chemistry of AIBN thermal decomposition. This resonator enables both simultaneous in situ heating using microwaves and EPR measurements to be performed. The thermal decomposition of AIBN was compared following conventional heating methods and microwave-induced (or dielectric) heating methods. Under both heating conditions, the radicals formed and detected by EPR include the 2-cyano-2-propyl (CP$^{\bullet}$) and 2-cyano-2-propoxyl (CPO$^{\bullet}$) radicals. Under aerobic conditions, the observed relative distribution of these radicals as observed by EPR is similar following slow heating by conventional or dielectric methods. In both conditions, the kinetically favoured CPO$^{\bullet}$ radicals and their adducts dominate the EPR spectra up to temperatures of approximately 80–90 °C. Under anaerobic conditions, the distribution can be altered as less CPO$^{\bullet}$ is available. However, the observed results are notably different when rapid heating (primarily applied using a MW-induced T-jump) is applied. As the higher reaction temperatures are achieved on a faster timescale, none of the ST$^{\bullet}$-CPO adducts are actually visible in the EPR spectra. The more rapid and facile heating capabilities created by microwaves may therefore lead to the non-detection of radical intermediates compared to experiments performed using conventional heating methods.

✉ Giuseppina Magri
MagriG@cardiff.ac.uk

✉ Andrea Folli
FolliA@cardiff.ac.uk

✉ Damien M. Murphy
MurphyDM@cardiff.ac.uk

[1] School of Chemistry, Cardiff University, Main Building, Park Place, Cardiff CF10 3AT, UK

[2] Centre for High Frequency Engineering, School of Engineering, Cardiff University, Cardiff CF24 3AA, UK

Keywords AIBN · EPR · Radicals · Spin trap · Resonator · Microwaves

Introduction

Conventional heating of liquids relies on the process of advection and diffusion to facilitate bulk heating. Upon initial heating of a liquid, molecules gain kinetic energy, moving throughout the liquid in random directions, thereby transferring heat via diffusion. This results in an overall reduction in the density of the liquid, allowing for advective transfer of heat energy to different regions within the liquid. Heat transfer from the source to the vessel containing the liquid and, in turn, to the liquid itself through this process is extremely slow and inefficient, resulting in potentially significant time delays before the entire sample volume reaches thermal equilibration. As such, conventional heating methods can be difficult to deploy if a homogenous instantaneous temperature jump (T-jump) is required, creating a rapid shift of a system away from thermodynamic equilibrium [1]. Such T-jumps are often employed in studies of reaction kinetics and chemical intermediates formed under non-equilibrium conditions.

As an alternative to conventional heating methods, microwave (dielectric) heating of liquids offers several advantages. In this case, the dielectric heating is achieved through two main mechanisms, namely ionic conduction and dipolar rotation [2]. The former is most applicable to ionic solutions, since the ions within the solution will align themselves with the oscillating electric field of the incident microwaves. The kinetic energy gained by these ions is lost via scattering as they flow, and as a result, heat is generated in the vicinity of each ion. Dipolar rotation on the other hand is also driven by the oscillating electric field but this time energy is dissipated as heat via the frictional forces arising from the inter-dipole bonds. Unlike conventional heating, dielectric heating induces an instantaneous, homogeneous temperature rise wherever a finite electric field is present, meaning that the bulk liquid can be heated volumetrically and rapidly to a higher temperature. It is therefore unsurprising that in recent years, a notable shift in the use of microwaves in chemical reaction engineering and synthesis has occurred [3–10]. Microwave heating has been reported to enhance the rate of chemical reactions and in some cases even increase the selectivity of products formed [11, 12], although there remains considerable controversy on how this is achieved [13–15].

The ability to use microwaves to thermally drive chemical reactions when combined with suitable techniques to study the intermediates formed is therefore most appealing. Chemical reactions often generate reactive short-lived radical intermediates that direct the transformation of reactants to products. If these intermediates can be more efficiently generated by microwave heating, then electron paramagnetic resonance (EPR) spectroscopy offers a suitable means to identify and understand the nature of the intermediates present, and their roles in any associated reactions. EPR detection at elevated temperatures can also give valuable information on the dynamics of paramagnetic species, whilst also enabling the reaction to be potentially monitored in situ. To this end, we have recently developed and tested two generations of a dual-mode EPR ‘reactor-resonator’ capable of simultaneous EPR detection and

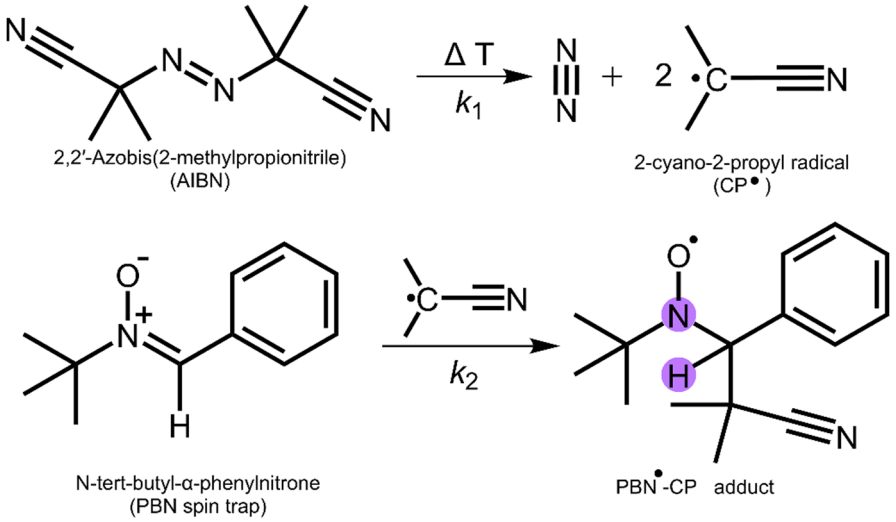

Scheme 1 Schematic illustration of the formation of the 2-cyano-2-propyl radical (CP$^{\bullet}$) and subsequent trapping by reaction with N-tert-butyl-α-phenylnitrone (abbreviated to PBN) following thermal decomposition of AIBN. The spin trapping reaction generates a persistent aminoxyl radical adduct (labelled PBN$^{\bullet}$-CP) that can be detected by CW-EPR spectroscopy. The highlighted atoms in the PBN$^{\bullet}$-CP adduct relate to the spin active nuclei that the unpaired electron will couple to and hence observe in the CW-EPR spectrum

microwave (MW)-induced dielectric heating [16, 17]. These resonators utilize two discrete microwave frequencies at *ca.* 9.5 GHz (magnetic field) for EPR detection and at *ca.* 6.1 GHz (electric field) for dielectric heating, making this an ideal resonator to monitor the 'real-time' in situ EPR response to dielectric heating [16, 17]. In this present study, we hereby demonstrate the utility and effectiveness of this resonator to monitor the radical formation via the thermal decomposition of 2,2′-azobis(2-methylpropionitrile) (hereafter labelled AIBN).

AIBN is a common azo compound widely used as a foaming agent in the plastics and rubber industries and commonly employed as a radical initiator in radical polymerizations [18–20]. When heated, the compound decomposes into N_2 and 2-cyano-2-propyl radicals (hereafter abbreviated to CP$^{\bullet}$ radicals); these radicals are capable of initiating the subsequent radical reactions. Owing to the highly reactive nature of CP$^{\bullet}$, including the tendency to form dimers, the use of a suitable spin trap agents (ST) becomes necessary for their detection by continuous wave (CW)-EPR (Scheme 1).

Many mechanistic studies of AIBN thermal decomposition have been published, using a variety of characterization or analytical techniques including EPR [21–23]. For example, it is well known that under aerobic conditions, these carbon-based CP$^{\bullet}$ radicals react with atmospheric oxygen to form a 2-cyano-2-propoxyl radical (hereafter abbreviated to CPO$^{\bullet}$ radical) as shown in Scheme 2.

For this reaction, a well-defined temperature dependency exists at which the oxygen- and carbon-based radicals are visible by EPR under aerobic conditions. For example, Janzen et al. [24] studied the thermolysis of AIBN under aerobic

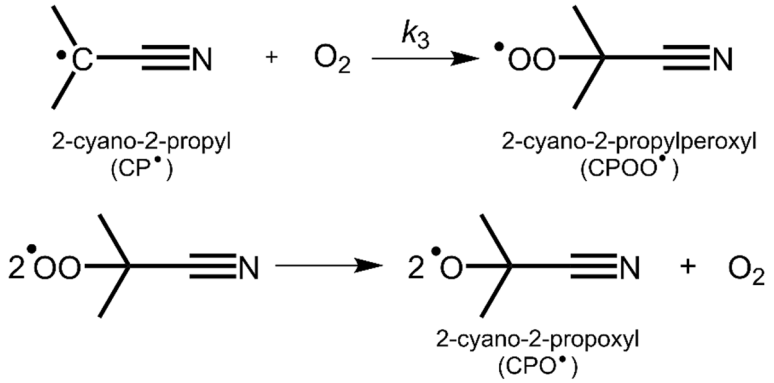

Scheme 2 Schematic illustration showing the formation of the 2-cyano-2-propoxyl (CPO$^{\bullet}$) radical

conditions at 65 °C utilizing PBN as the ST and observed only a PBN$^{\bullet}$-CPO adduct when conventional heating methods were used. The carbon-based PBN$^{\bullet}$-CP adduct was only observed at higher temperatures. Indeed, the generation of these radicals has also been examined by other external stimuli that induce AIBN decomposition, such as UV-irradiation and laser flash photolysis [24–26]. Nevertheless, despite this widely studied reaction, the effects of dielectric heating as a source of thermal decomposition step, coupled with EPR detection, have never been explored to date despite the increasing use of microwave reactors in laboratory syntheses.

In this paper, the differences between conventional and dielectric heating on the thermal decomposition of AIBN will therefore be presented using a custom-built dual-mode EPR resonator. The thermal decomposition of AIBN offers an ideal model reaction for investigating some generic differences between standard conventional heating techniques and dielectric heating on radical reactions as detected by EPR spectroscopy.

Experimental details

Sample preparation under aerobic conditions

Commercially available AIBN (supplied as a solid compound) was purchased from Sigma-Aldrich (CAS: 78-68-1) and used as received. The compound was dissolved in toluene or *o*-xylene solution resulting in a 20 mM AIBN stock solution. To this stock solution, 3 eq. of PBN (N-tert-butyl-α-phenylnitrone, CAS: 3376-24-7) or DMPO (5,5-dimethyl-1-pyrroline N-oxide, CAS: 3317-61-1) purchased from TCI, was added directly to the solution, hereafter referred to as the AIBN/PBN or AIBN/DMPO solution. A 100 µl aliquot of this solution was loaded into a quartz Q-band EPR tube (product number: WG-221 T-RB Wilmad Labglass, O.D = 1.6 mm and I.D = 1.1 mm) and placed within the active MW field of the resonator. The resulting stock solution of AIBN, spin trap (ST) in toluene or *o*-xylene was refrigerated.

Sample preparation under anaerobic conditions

Dry toluene was degassed via the freeze-pump thaw method to remove O_2 and transferred into a glovebox. A dried and degassed solution of 3 eq. DMPO in toluene solution was transferred into the glovebox operating under an Ar atmosphere, prior to addition to a 20 mM AIBN toluene solution. 100 µl aliquots of AIBN solution containing DMPO were subsequently transferred into Q-band tubes and sealed with high vacuum grease and Teflon tape. For partially degassed samples, the AIBN/DMPO/Toluene solutions were prepared under aerobic conditions and stopped with a rubber cap. A needle connected to an Ar lecture bottle was inserted into the solution and bubbled with Ar for 3 or 4 min.

Heating procedures

The variable temperature (VT) heating and EPR studies were carried out by flowing hot N_2 gas through a quartz insert mounted inside a Bruker super-high Q resonator (ER4122-SHQE) connected to a Bruker N_2 transfer arm. A thermocouple placed inside the quartz insert was used to measure the temperature. A mass flow meter (GE250A, mks instruments) attached to a mass flow controller (model number: 946, mks instruments) was used to control the N_2 flow. Hereafter, this use of flowing hot N_2 gas through the Bruker resonator to heat the sample is referred to as the conventional heating method. In addition, rapid temperature increases under conventional methods conditions were achieved using the highest gas flow possible (0.08 L/min, see Supporting Information). The variable temperature (VT) heating and EPR studies were also carried out using microwaves in our custom designed and built dual-mode EPR resonator (details of resonator construction can be found in our earlier publications [16, 17]); hereafter, this use of microwaves is referred to as the dielectric heating method. A fibre-optic probe (LumaSense LUXTRON 812 Industrial Temperature Monitor equipped with a MicroProbe) was used for temperature measurement. A given desired temperature was achieved by tuning the power of the *ca.* 6.1 GHz microwave frequency in the resonator to optimize and maximize the heating rate. The power applied to the dual-mode resonator when loaded with the sample of AIBN/PBN/Toluene for the T-jump measurements was 444 mW and for the AIBN/DMPO/Toluene sample, 329 mW (see Supporting Information). For the *o*-xylene T-jump measurements, a power of 799 mW was used for the AIBN/PBN/*o*-xylene sample and 729 mW for the AIBN/DMPO/*o*-xylene sample.

EPR measurements

EPR spectra were recorded on a Bruker EMX spectrometer operating at 100 kHz field modulation frequency; 0.1 mT field modulation amplitude; 5.12 ms time constant; 10.24 ms conversion time. Spectra were signal averaged over five scans. The receiver gain (RG) was selected as required for each measurement, resulting from differences in sensitivity between cavities. Ordinarily, when utilizing the Bruker

SHQE resonator (ER4119-SHQE), a RG of 1×10^4 was typically used, but with our home built dual-mode resonator, a RG of 1×10^5 was employed. The T-jump experiments were acquired via 2D EPR experiment set-ups, using two scans per slice, resulting in 100 slices, recorded using 0.32 ms time constant and conversion time. All CW-EPR spectra were simulated using the EasySpin [27] MATLAB toolbox.

Results

EPR spectra recorded under variable temperature heating conditions

In order to monitor the distribution of radical adduct formation over a given temperature range, following AIBN thermal decomposition, and to compare this product distribution for conventional heating versus dielectric heating, a series of variable temperature EPR measurements were performed. In the initial series of experiments, aerobic solutions of AIBN containing a ST (either PBN or DMPO) were heated to various temperatures, and in all cases, the CW-EPR spectra were simultaneously recorded at these elevated temperatures. Sample heating was achieved either using the conventional methods or the dielectric heating methods as described above in the experimental section. The resulting CW-EPR measurements are shown in Fig. 1. The overall spectral profiles recorded under both conventional and dielectric heating conditions suggest that, within a tolerance difference of ± 5 °C, both heating methods produce a similar distribution of trapped radicals (CP$^\bullet$ or CPO$^\bullet$). Qualitative analysis of the EPR spectra and identification of the resulting trapped radicals are achieved by comparing the experimental EPR parameters (isotropic ^{1}H and ^{14} N hyperfine coupling constants, a_{iso}) to previously published values (Table 1).

As previously mentioned, the carbon-based CP$^\bullet$ radicals formed by initial decomposition of the AIBN molecule react quickly with atmospheric oxygen to form a peroxyl radical, that readily decomposes to produce a propoxyl CPO$^\bullet$ radical, as shown in Scheme 2. The spin trap adduct of the 2-cyano-2-propylperoxyl (CPOO$^\bullet$) radical was never detected in this work, as expected since this reactive adduct is known to be very temperature sensitive and has never been observed by EPR above 230 K [24].

The EPR spectra recorded using PBN as the ST indicate that the EPR signal intensity grows with increasing temperature up to 85 °C (under conventional heating) and up to 80 °C (under MW heating) (Fig. 1a, c), with only a minor change observed in the line shapes due to the simultaneous presence of the two radical adducts (i.e. ST$^\bullet$-CP and ST$^\bullet$-CPO) (Table 2). The values of the hyperfine coupling constants in Table 1 confirm that the radical species detected at 80 °C by conventional heating (or at 75 °C by MW heating) can be easily assigned to a PBN$^\bullet$-CPO adduct. As the temperature is raised above 90 °C, only the PBN$^\bullet$-CP adduct is observed, regardless of whether conventional or dielectric heating was employed.

An identical series of results were obtained using the second ST (DMPO) as shown in Fig. 1b, d, with a mixture of both ST$^\bullet$-CP and ST$^\bullet$-CPO observed. In this case, the EPR spectra contained the highest contribution from the DMPO$^\bullet$-CPO adduct at temperatures up to 90 °C (via conventional heating) or 85 °C (via

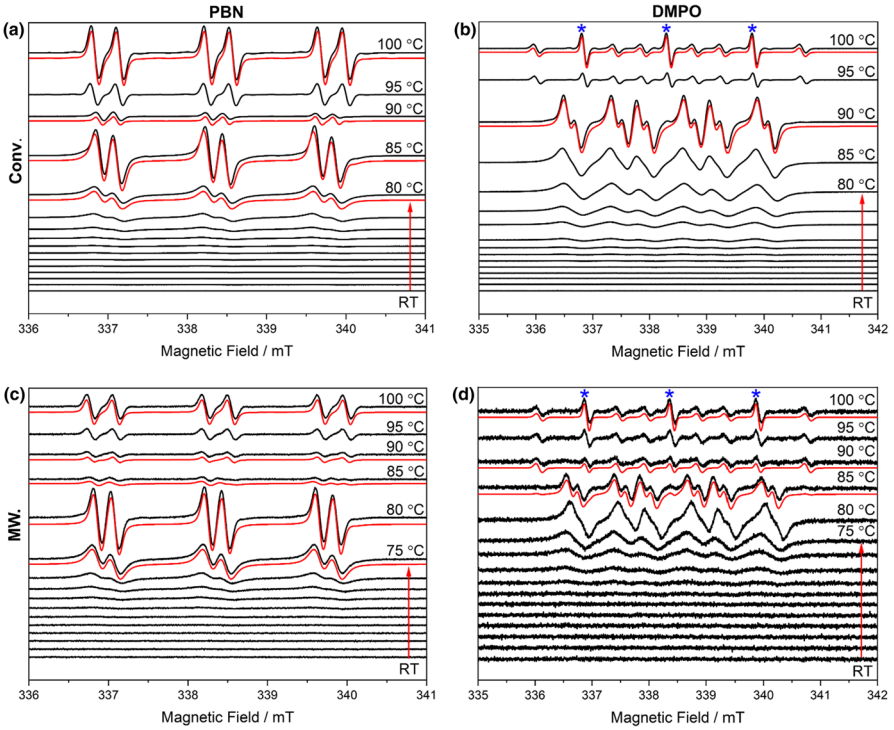

Fig. 1 Variable temperature X-band CW-EPR spectra of a 20 mM AIBN solution under aerobic conditions containing **a**, **c** 3 eq. PBN and **b**, **d** 3 eq. DMPO in toluene. The increase in sample temperature was achieved via conventional heating (results shown in a, b) or dielectric heating (results shown in **c**, **d**. The red lines indicate simulated EPR spectra. Blue asterisks indicate EPR resonances associated with degraded DMPO

microwave heating). At higher temperatures, $T \geq 90$ °C, the DMPO$^{\bullet}$-CP adduct becomes most dominant (Tables 1 and 2). Interestingly, simulations of EPR spectral contributions (reported in Table 2) indicate a greater contribution of CP$^{\bullet}$ radicals compared to CPO$^{\bullet}$ radicals for samples treated to dielectric heating at each interrogated temperature.

EPR measurements performed under anaerobic conditions

The reaction pathway for generating the CP$^{\bullet}$ and CPO$^{\bullet}$ radicals (see Schemes 1 and 2), and the reason why the CPO$^{\bullet}$ radicals dominate the EPR spectra at lower temperatures must be carefully considered. In the previous experiments (Fig. 1), the observations were made using aerobic solutions. However, the mechanism for radical formation, and in particular the role of molecular oxygen, can be further interrogated by performing the conventional heating experiments under anaerobic conditions (either with partially or fully degassed solutions of AIBN/DMPO/Toluene). The results of the thermal decomposition experiments performed using

Table 1 Spin Hamiltonian parameters (g_{iso} and a_{iso}) for the PBN/DMPO-radical adducts formed via AIBN decomposition; the parameters were extracted by simulation of the EPR spectra

Spin trap	Radical trapped	a^N	a^H	[a]Other	g_{iso}	Solvent	Refs.
PBN	CP$^\bullet$	1.433	0.312	^{13}C = 1.075	2.0058	Toluene	t.w
PBN	CP$^\bullet$	1.430	0.322	–	2.0059	Benzene	[24]
PBN	CP$^\bullet$	1.460	0.307	–	–	THF	[28]
PBN	CPO$^\bullet$	1.387	0.206	–	2.0062	Toluene	t.w
PBN-d_9	CPO$^\bullet$	1.387	0.206	–	2.0061	Benzene	[24]
PBN-nitronyl-^{13}C	CPO$^\bullet$	1.393	0.216	^{13}C = 0.470	–	Benzene	[25]
DMPO	CP$^\bullet$	1.390	1.875	^{14} N = 1.485	2.0059	Toluene	t.w
DMPO	CP$^\bullet$	1.460	2.040	–	–	Xylene	[28]
DMPO	CPO$^\bullet$	1.275	0.827	^{1}H = 0.165	2.0058	Toluene	t.w
DMPO	CPO$^\bullet$	1.266	0.837	^{1}H = 0.189	–	Benzene	[24]
*MNPE	CP$^\bullet$	1.485	–	–	2.0058	Toluene	t.w
'DMPO-deg'	N/A	1.480	–	–	2.0040	Water	[29]
'DMPO-deg'	N/A	1.490	–	–	–	DMSO	[30]

All hyperfine values are given in units of mT. *MNPE = 4-methyl-4-nitroso-pentanal. The MNPE$^\bullet$-CP adduct is formed through the breakdown of DMPO$^\bullet$-CPO, as shown in Scheme 4

Table 2 EPR spectral contributions of radical adducts detected in the VT EPR study shown in Fig. 1

Heating method	Spin trap	Temp./°C	% of ST$^\bullet$-CPO	% of ST$^\bullet$-CP	% degraded DMPO
Conventional	PBN	80	100	0	N/A
		85	100	0	N/A
		90	60	40	N/A
		100	0	100	N/A
Dielectric	PBN	75	100	0	N/A
		80	90	10	N/A
		85	37	63	N/A
		90	13	87	N/A
		100	0	100	N/A
Conventional	DMPO	90	100	0	0
		100	0	50	50
Dielectric	DMPO	85	98	1	1
		90	0	80	20
		100	0	50	50

The percentages of adducts present were calculated through the simulated weighting of contributions to the EPR spectra

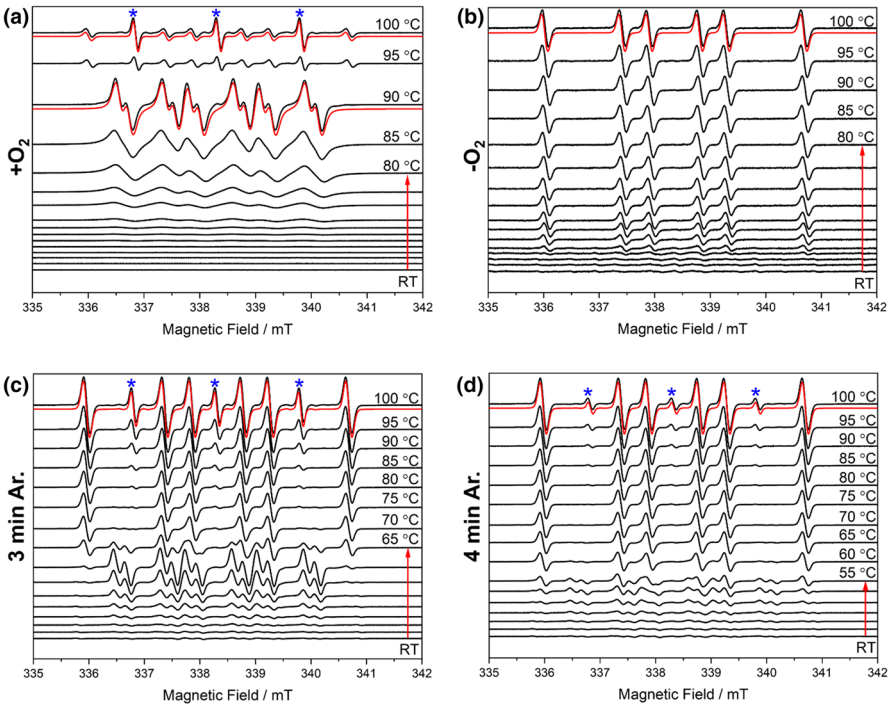

Fig. 2 Variable temperature X-band CW-EPR spectra of a 20 mM AIBN solution with 3 eq. DMPO in aerobic, anaerobic and partially degassed solutions; **a** aerobic conditions (previously shown in Fig. 1b), **b** fully anaerobic conditions, and c, d partially anaerobic conditions, specifically **c** after 3 min of Ar bubbling through the solution and **d** after 4 min of Ar bubbling. The sample temperature was increased by conventional heating in all cases

anaerobic conditions are presented in Fig. 2. In these experiments, the DMPO ST was chosen over PBN, simply because DMPO affords better spectral profiles differences and hyperfine couplings between the two adducts (i.e. easier to discriminate between the two radicals using DMPO compared to PBN).

Under fully anaerobic conditions (Fig. 2b), only the DMPO$^{\bullet}$-CP adduct was observed at all temperatures as expected (i.e. with no oxygen available in solution, the carbon-based radicals cannot react with O_2 to produce CPO$^{\bullet}$). However, under partially degassed conditions, the product distribution over the interrogated temperature range was notably different due to the now limited supply of O_2. Under fully aerobic conditions, the signal from the DMPO$^{\bullet}$-CP adduct could not been seen at temperatures below 95 °C (Fig. 2a), as these lower temperature spectra are dominated by contributions from DMPO$^{\bullet}$-CPO. However, in the partially degassed solutions, this DMPO$^{\bullet}$-CP adduct signal was now clearly visible at the lower temperatures (65 °C and 55 °C, in Fig. 2 c, d respectively) owing to the smaller intensity of the DMPO$^{\bullet}$-CPO. The DMPO$^{\bullet}$-CPO signal completely disappears at 70 °C after 3 min of Ar bubbling through the solution and at 65 °C

after 4 min (Fig. 2c, d), where previously in fully aerobic conditions (Fig. 2a), this signal disappeared above 90 °C.

Rapid heating (T-jump) measurements

The relative abundances of the carbon- and oxygen-based radicals, namely $CP^{\bullet}$ and $CPO^{\bullet}$, are important for radical polymerization, as the former act as radical initiators, whilst the latter act as chain terminators. The relative kinetics of radical formation is very different in this case, as is the experimental temperature window in which they can be observed. One must therefore be careful when drawing any conclusions on radical abundances based on the available technique used to study or quantify them. To explore this issue further, the heating experiments for AIBN decomposition were subjected to a sudden and rapid rise in temperature (i.e. a temperature jump) as opposed to the slow continuous heating conditions applied earlier. This experiment enables one to explore any changes in observed radical adduct signal intensities following the rapid temperature jump in the solution.

In these rapid heating (T-jump) experiments, the solution was allowed to equilibrate to room temperature for 2 min before initiating the mode of heating (Fig. 3).

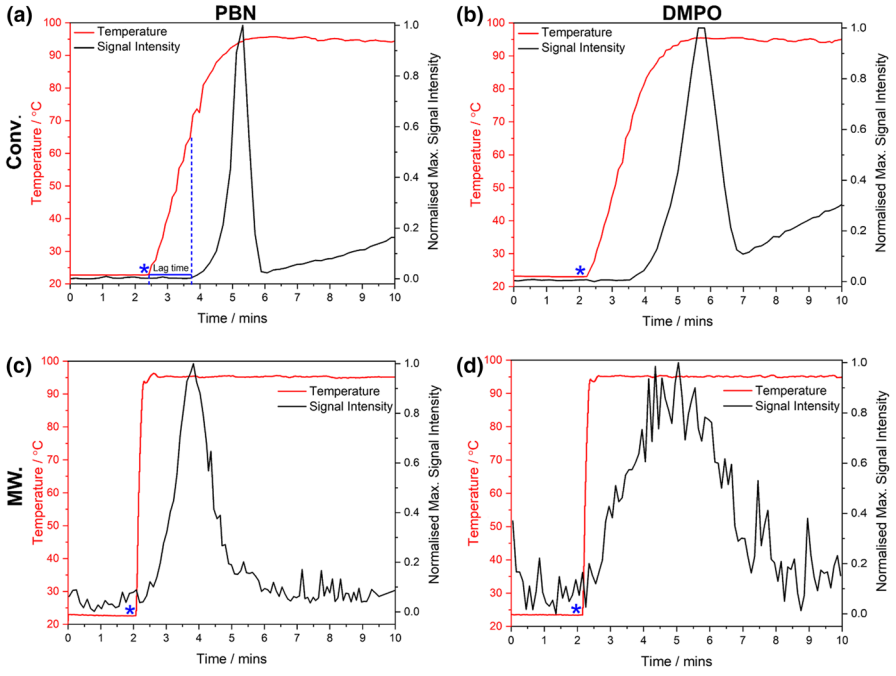

Fig. 3 Changes to the spin adduct EPR signal intensity as a function of time following a rapid temperature rise (T-jump) in a 20 mM AIBN aerobic solution containing **a**, **c** 3 eq. PBN and **b**, **d** 3 eq. DMPO in toluene. The rapid temperature increases were induced by **a**, **b** conventional heating (by increasing the N_2 flow rate) or **c**, **d** dielectric heating (note the more rapid, sharp rise in temperature in this MW heating case). The blue asterisks indicate initiation of heating

The target temperature of 95 °C was reached after *ca.* 3 min using conventional heating (Fig. 3a, b), but after only 30 secs using dielectric heating (Fig. 3c, d). This target temperature was chosen since only the signal of the trapped ST$^{\bullet}$-CP adduct should remain visible at these high temperatures (as shown earlier in Fig. 1). The integrated EPR signal intensity is plotted in Fig. 3 (labelled Normalized Maximum Signal Intensity). It should be stated that although the overall EPR signal is dominated by contributions from the trapped CPO$^{\bullet}$ radical, a small contribution will nevertheless come from the trapped CP$^{\bullet}$ radical (i.e. both radicals contribute to the overall integrated intensity). Owing to the faster heating rates achieved using dielectric heating compared to conventional heating, the lag time between the temperature initiation point and the first appearance of an EPR signal is correspondingly shorter using microwaves (*ca*. 7 and 6 secs for PBN and DMPO adducts, respectively, Fig. 3c, d) compared to conventional heating (*ca*. 75 secs for both adducts, Fig. 3a, b). On a technical point, separate multifrequency dielectric measurements on the solution permittivity were conducted and these revealed that the loss of the DMPO solution is greater than the PBN solutions by *ca.* 6% (see Supporting information for details). This explains the small discrepancy in applied power and thus heating rates for the PBN vs DMPO solutions.

The results in Fig. 3 clearly indicate an increase in signal intensity up to the target temperature point, and beyond this, the signal intensity rapidly drops off. At this point, only the small residual component from the trapped CP$^{\bullet}$ radical remains and contributes to the signal intensity. The drop off in signal intensity is clearly associated with the loss in ST$^{\bullet}$-CPO adduct abundance. As discussed later, various reactions are responsible for the loss of the ST$^{\bullet}$-CPO adduct. Figure 3 c,d indicates that although achieving a faster rate of heating when utilizing dielectric heating, the ST$^{\bullet}$-CPO adduct is still visible. This point was further illustrated by enhancing the target temperature to 135 °C, over a similar timescale. For these experiments, solutions were prepared in *o*-xylene (as opposed to toluene, which will boil above 110 °C). Under these conditions, no signal of the PBN/DMPO$^{\bullet}$-CPO adducts was detected (Fig. 4). Despite the normal radical chemistry of CPO$^{\bullet}$ still occurring, the EPR signals are completely absent in Fig. 4 (and only moderately visible

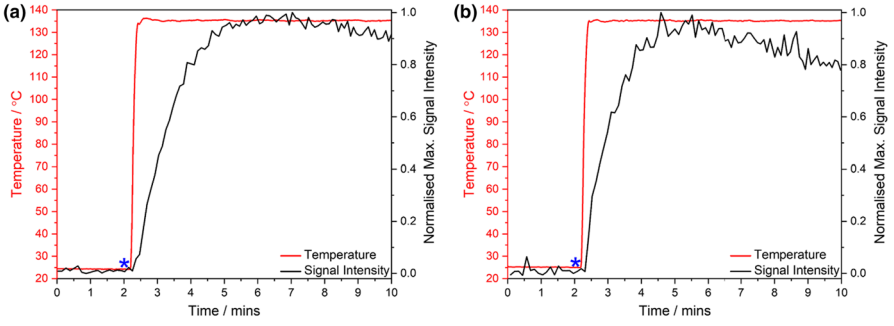

Fig. 4 Monitoring the signal intensity and temperature as a function of time for 20 mM AIBN under aerobic conditions with **a** 3 eq. PBN and **b** 3 eq. DMPO in *o*-xylene, temperature increased via dielectric heating

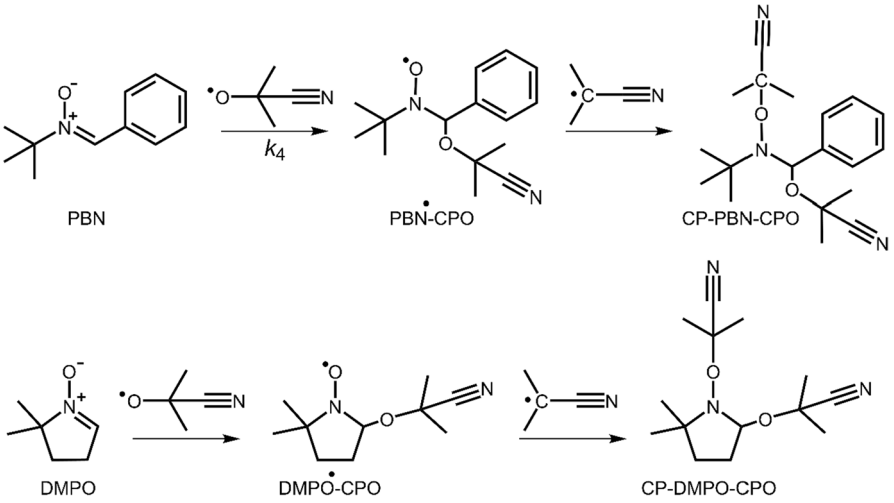

Scheme 3 Formation of the diamagnetic mixed alkoxyamine

in Fig. 3) simply because the rate of heating was so fast. The target temperature of 135 °C is reached within *ca.* 20 secs utilizing AIBN/PBN/*o*-xylene, whilst for AIBN/DMPO/*o*-xylene, this time is slightly reduced to *ca.* 15 secs. The lag time of the PBN- and DMPO$^{\bullet}$-CP adducts in *o*-xylene were 4 secs and 7 secs, respectively. In other words, conventional heating enables the ready observation of these radicals, as their abundance builds up in solution, whereas rapid dielectric heating does not facilitate their detection by EPR (i.e. their formation and subsequent decay occur quickly, so no signal can be observed).

Discussion

VT measurements (origin of the CPO$^{\bullet}$ radical at T ≤ 90 °C)

The thermal decomposition of AIBN results in the formation of CP$^{\bullet}$ radicals (Scheme 1), with formation rates of $k_1 = 0.4 \times 10^4$ s^{-1} at 70 °C and $k_{1'} = 16 \times 10^4$ s^{-1} at 100 °C [31]. This is much slower compared to the reaction of CP$^{\bullet}$ with molecular oxygen forming the CPOO$^{\bullet}$ radical (with a second-order rate constant of $k_3 = 4.9 \times 10^9$ M^{-1} s^{-1}) [32]. This peroxyl radical can further react to generate a CPO$^{\bullet}$ radical (Scheme 2) which is subsequently trapped by the ST and detected via EPR. At elevated temperatures (above *ca.* 85–90 °C for conventional heating or 80–85 °C for MW heating), the EPR signal intensity clearly decreases. The loss in signal can at least be partially attributed to mixed adduct formation. Using liquid chromatography–mass spectrometry (LC/MS), Janzen et al. [24] proved that under aerobic conditions, after an extended thermolysis of AIBN (using PBN) between 65 and 110 °C and AIBN (using DMPO) at 75 °C, a CP-PBN-CPO or CP-DMPO-CPO diamagnetic mixed adduct can be formed (i.e. an alkoxyamine, see Scheme 3).

This observation explains the loss of the ST$^{\bullet}$-CPO adduct EPR signal intensity at these higher temperatures (Scheme 3). It is also important to note that Guo et al. [33] studied the thermal decomposition of AIBN into its associated radial products at various temperatures. The conversion at 80 °C was found to be 0.6 after 5 h; at 85 °C, the conversion was 0.6 after 2 h; and at 100 °C, the conversion was 0.9 after 0.9 h. Therefore, it was concluded that AIBN is likely to undergo complete thermal decomposition, and specifically, the conversion will not reach 1.

As illustrated in Scheme 2, once the CP$^{\bullet}$ radical is generated, the reaction with molecular oxygen to form CPO$^{\bullet}$ exhibits fast reaction kinetics [32]. The rate of addition of a *t*-butoxyl radical to PBN is reported to be $k_4 = 5.5 \times 10^6$ M^{-1} s^{-1} [34] (for which CPO$^{\bullet}$ can be compared to) which is one hundred times faster than the rate of addition of a *t*-butyl radical to PBN, i.e. $k_2 = 1 \times 10^4$ / M^{-1} s^{-1} (for which CP$^{\bullet}$ can be compared to) [24]. Therefore, it is not surprising that the first signal seen in the variable temperature EPR spectra (Fig. 1a–d) is due to the ST$^{\bullet}$-CPO adduct, owing to the more favourable reaction kinetics leading to a higher abundance of the radical and subsequent accumulation of this adduct.

Aerobic versus anaerobic experimental considerations

The results presented in Fig. 2 directly arise from a reduced competition for the ST in the absence of excess oxygen (in which CPO$^{\bullet}$ radicals cannot form). Interestingly, the triplet signal characteristic of degraded DMPO is not seen at all under anaerobic conditions. The signal intensity for the DMPO$^{\bullet}$-CP adduct is lower than that of the DMPO$^{\bullet}$-CPO adduct and the degraded DMPO signal (Fig. 2a). The slow degradation kinetics of AIBN should facilitate the formation of both DMPO$^{\bullet}$-CPO and DMPO$^{\bullet}$-CP over the full temperature range. However, as the rate of the CPO$^{\bullet}$ radical addition to the ST exceeds that for CP$^{\bullet}$, it is likely that CPO$^{\bullet}$ is trapped in excess relative to CP$^{\bullet}$ giving rise to a dominant EPR signal observed under aerobic conditions. At higher temperatures ($T > 90$ °C), the DMPO$^{\bullet}$-CPO adduct is clearly not stable, hence, no EPR signal is detected. Simulation of the experimental spectra reveals a higher percentage of 'degraded' DMPO when the sample is degassed for 3 min (15%) compared to 4 min (6%) (Fig. 2c,d) as there is a higher concentration of oxygen and thus DMPO$^{\bullet}$-CPO adducts to ring-open and decompose. A proposed ring opening mechanism is presented in Scheme 4.

Scheme 4 suggests an extra contribution to the loss of the adduct signal at higher temperatures, involving a breakdown of the DMPO$^{\bullet}$-CPO adduct to form 4-methyl-4-nitroso-pentanal (MNPE) and a CP$^{\bullet}$ radical. MNPE can act as a ST itself via the nitroso moiety. Therefore, the available CP$^{\bullet}$ radicals (formed either from direct thermal decomposition of AIBN (Scheme 1) or from thermal decomposition of DMPO$^{\bullet}$-CPO (Scheme 4)) can generate the MNPE$^{\bullet}$-CP adduct, whereby only the hyperfine coupling, $a_{iso}(^{14}N)$ (indicated by blue asterisks, Figs. 1 and 2), is observed, as well as DMPO$^{\bullet}$-CP.

Following the degradation of the DMPO$^{\bullet}$-CPO adduct, the thermally stable DMPO$^{\bullet}$-CP adduct then appears to dominate in the solution and appears in a high

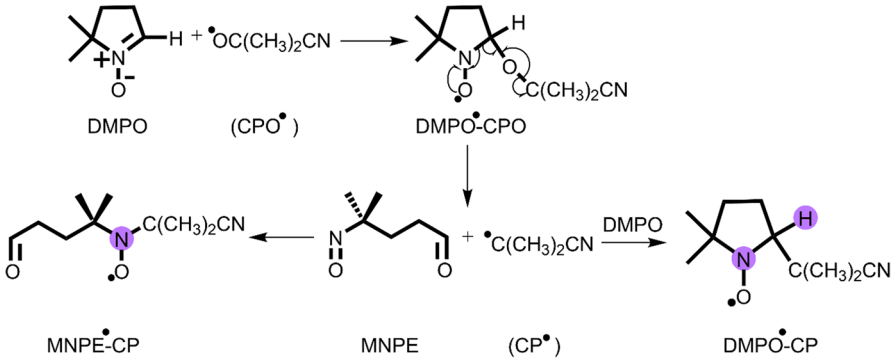

Scheme 4 Decomposition of DMPO•-CPO into MNPE. Adapted from Ref. [30] MNPE represents the secondary indirect ST formed in the degradation of DMPO•-CPO

enough concentration to be detected via EPR, albeit with a lower intensity compared to the initial DMPO•-CPO adduct (Fig. 2a).

Loss of radical signals following T-jump measurements

Rapid heating of the solution using a T-jump results in a notably different set of observables in the experimental EPR spectra. Using both heating methods, up to *ca*. 95 °C, the more dominant ST•-CPO adduct appears in the EPR spectra (Fig. 3). Beyond the maximum signal intensity, the signal rapidly disappears due to loss in abundance of the adduct, resulting from decomposition for example, with trace amounts of the ST•-CP signal being observed towards the end of the monitored reaction timescale. However, when the sample is rapidly heated dielectrically to 135 °C (Fig. 4), no signal associated with ST•-CPO is observed, and instead only the ST•-CP adduct is solely detected by EPR. As stated above, this is attributed to the degradation of DMPO•-CPO, and/or the formation of a mixed diamagnetic double adduct (CPO-PBN/DMPO-CP alkoxyamine). An observed minor decrease in signal intensity of the two adducts at *ca.* 7 min (Fig. 4) can be attributed to the potential formation of another diamagnetic alkoxyamine species [35], where the nitroxide moiety can react with another CP• radical similar to Scheme 3 forming CP-PBN/DMPO-CP. By dielectrically heating at an increased rate to a higher target temperature, we have demonstrated the complete avoidance of the ST•-CPO EPR signal.

The absence of detectable ST•-CPO adducts in the EPR spectra following a rapid rise in temperature does not imply that the radicals are not formed. Rather, it merely indicates that as the higher temperatures are achieved on a faster timescale (between 15 and 20 secs in Fig. 4 using a MW-induced T-jump compared to the slower conventional heating methods in Fig. 3a, b), the CPO• radicals and their spin trapped adducts have already formed and decayed, so are no longer observable by EPR. As microwave reactors become more commonplace in synthetic laboratories, the potential to achieve target reaction temperatures more quickly, compared to conventional

heating methods, should be carefully considered when interpreting the results of any underlying reaction mechanism. In other words, the lack of any observed product or radical could be misinterpreted as an absence of that product or radical from the reaction mechanism, rather than the faster intrinsic heating rate afforded by microwaves preventing the steady-state build-up of accumulation of adducts detected by EPR. Such rapid heating conditions, and their influence on the detectable experimental observables, can easily be overlooked.

Conclusion

The thermal decomposition of AIBN using conventional and microwave (dielectric) heating leads to the formation of carbon- and oxygen-based radicals. These short-lived radicals can be trapped by a suitable ST agent and the resulting long-lived adducts studied by EPR. In this study, the dielectric heating was performed using a custom-built dual-mode EPR resonator which enables simultaneous heating and EPR detection experiments to be performed. This resonator also offers the ability to directly study in situ the radical chemistry of microwave-induced AIBN decomposition, as opposed to the slower conventional heating methods that standard EPR resonators rely upon. Owing to the rate of O_2 addition to the $CP^{\bullet}$ radical (and the rapid addition of $CPO^{\bullet}$ to the PBN ST), the kinetically favoured $CPO^{\bullet}$ radicals and their adducts dominate the reaction medium and the resulting EPR spectra up to temperatures of approximately 80–90 °C. The primary but kinetically unfavoured $CP^{\bullet}$ radicals are barely visible in the EPR spectra. However, at elevated temperatures, a rapid loss in signal intensity associated with the $ST^{\bullet}$-CPO spin adduct occurs, enabling the $ST^{\bullet}$-CP spin adduct signal to be observed. This signal from the carbon-based species can also be readily detected under anaerobic conditions. Crucially, this kinetically controlled chemistry, and associated thermal stabilities of the resulting adducts, is all observed under conventional or ‘slow’ heating conditions. On the other hand, rapid heating (applied via a MW-induced T-jump) of the solution using microwave heating enables the higher reaction temperature to be achieved on a faster timescale. Under such conditions, none of the $ST^{\bullet}$-CPO adducts are actually visible in the EPR spectra, despite their presence in solution and regardless of their detection by EPR when the solution is heated by conventional means. The more rapid and facile heating capabilities created by microwaves may therefore lead to the non-detection of radical intermediates compared to experiments performed using conventional heating methods, and such observations must be carefully considered when studying radical-based mechanisms in solution using microwave heating sources.

Supplementary Information The online version contains supplementary material available at https://doi.org/10.1007/s11164-022-04861-z.

Author contributions The microwave engineers MB, HC, DS and AP (Cardiff University School of Engineering) were responsible for designing and constructing the dual-mode EPR resonator. The EPR spectroscopy team, GM, JF-C, ER, AF and DM (Cardiff University School of Chemistry), was responsible

for testing the resonator and performing all the EPR measurements reported. All authors contributed to writing and reviewing the manuscript.

Funding The authors thank the EPSRC (EP/R04483X) for financial support.

Data availability The data that support the findings of this study are available on the Cardiff University Research Portal (https://doi.org/10.17035/d.2022.0226041954) or from the corresponding authors upon reasonable request.

Declarations

Conflict of interest The authors declare no personal or financial interests that are directly or indirectly related to this work submitted for publication.

Ethical approval Not applicable.

References

1. Eigen, Norrish, and Porter, *Chemistry Nobel Prize* (1967).
2. P.A. Mello, J.S. Barin, R.A. Guarnieri, Microwave heating, in *Microwave-assisted sample prepared trace element determined*. ed. by E. de Marlon, M. Flores (Elsevier, Amsterdam, 2014), pp.59–75
3. J.L. Carden, L.J. Gierlichs, D.F. Wass, D.L. Browne, R.L. Melen, Chem. Commun. **55**, 318 (2019)
4. X. Wu, Z. Wang, D. Zhang, Y. Qin, M. Wang, Y. Han, T. Zhan, B. Yang, S. Li, J. Lai, L. Wang, Nat. Commun. **12**, 1 (2021)
5. J. Zhu, J. Zhang, R. Lin, B. Fu, C. Song, W. Shang, P. Tao, T. Deng, Chem. Commun. **57**, 12611 (2021)
6. S. Reynaud, B. Grassl, Adv. Polym. Sci. **274**, 131 (2016)
7. C.O. Kappe, Angew. Chem. Int. Ed. **43**, 6250 (2004)
8. A.G.R. Howe, R. Maunder, D.J. Morgan, J.K. Edwards, Catalysts **9**, 1 (2019)
9. M. Henary, C. Kananda, L. Rotolo, B. Savino, E.A. Owens Ab, G. Cravotto, RSC Adv. **10**, 14170 (2020)
10. S. Głowniak, B. Szczęśniak, J. Choma, M. Jaroniec, Adv. Mater. **33**, 1 (2021)
11. S. Horikoshi, J. Tsuzuki, M. Kajitani, M. Abe, N. Serpone, N. J. Chem. **32**, 2257 (2008)
12. J. Zhou, W. Xu, Z. You, Z. Wang, Y. Luo, L. Gao, C. Yin, R. Peng, L. Lan, Sci. Rep. **6**, 1 (2016)
13. C.O. Kappe, B. Pieber, D. Dallinger, Angew. Chem. Int. Ed. **52**, 1088 (2013)
14. G.B. Dudley, R. Richert, A.E. Stiegman, Chem. Sci. **6**, 2144 (2015)
15. D. Obermayer, B. Gutmann, C.O. Kappe, Angew. Chem. Int. Ed. **48**, 8321 (2009)
16. A. Folli, H. Choi, M. Barter, J. Harari, E. Richards, D. Slocombe, A. Porch, D.M. Murphy, J. Magn. Reson. **310**, 1 (2020)
17. M. Barter, G. Magri, J. Harari, H. Choi, A. Folli, D.R. Slocombe, E. Richards, D.M. Murphy, A. Porch, Appl. Magn. Reson. **53**, 861 (2022)
18. S.H. Liu, Y.P. Yu, Y.C. Lin, S.Y. Weng, T.F. Hsieh, H.Y. Hou, J. Therm. Anal. Calorim. **116**, 1361 (2014)
19. V. Sciannamea, C. Guerrero-Sanchez, U.S. Schubert, J.M. Catala, R. Jérôme, C. Detrembleur, Polym. (Guildf). **46**, 9632 (2005)

20. L. Fang, G. Han, H. Zhang, Adv. Polym. Sci. **274**, 87 (2016)
21. V. Sciannamea, J.M. Cátala, R. Jerome, C. Jérôme, C. Detrembleur, J. Polym. Sci. Part A Polym. Chem. **47**, 1085 (2009)
22. X.R. Li, X.L. Wang, H. Koseki, J. Hazard. Mater. **159**, 13 (2008)
23. T. Kunitake, S. Murakami, Polym. J. **3**, 249 (1972)
24. E.G. Janzen, P.H. Krygsman, D. Larry Haire, D.A. Lindsay, J. Am. Chem. Soc. **112**, 8279 (1990)
25. D. Lawrence Haire, U.M. Oehler, P.H. Krygsman, E.G. Janzen, J. Org. Chem. **53**, 4535 (1988)
26. A.N. Savitsky, H. Paul, J. Phys. Chem. A **104**, 9091 (2000)
27. S. Stoll, A. Schweiger, J. Magn. Reson. **178**, 42 (2006)
28. M. Iwamura, N. Inamoto, Bull. Chem. Soc. Jpn. **43**, 860 (1970)
29. L. Ghassemzadeh, T.J. Peckham, T. Weissbach, X. Luo, S. Holdcroft, J. Am. Chem. Soc. **135**, 2 (2013)
30. E. Finkelstein, G.M. Rosen, E.J. Rauckman, Mol. Pharmacol. **21**, 262 (1982)
31. M. Talat-Erben, S. Bywater, Trans. Faraday Sac. **71**, 2027(1949)
32. P. Nata, R.E. Huie, A.B. Ross, J. Phys. Chem. Ref.Data. **19**, 413 (1990)
33. S. Guo, W. Wan, C. Chen, W.H. Chen, J. Therm. Anal. Calorim. **113**, 1169 (2013)
34. E.G. Janzen, A.C. Evans, J. Am. Chem. Soc. **95**, 8205 (1973)
35. S. Matsumura, A.R. Hlil, C. Lepiller, J. Gaudet, D. Guay, Z. Shi, S. Holdcroft, A.S. Hay, J. Polym. Sci. Part A Polym. Chem. **46**, 7207 (2006)